

AD-A038 680

MARYLAND UNIV COLLEGE PARK DEPT OF PHYSICS AND ASTRONOMY F/G 20/8
ELASTIC AND INELASTIC CONTRIBUTIONS TO THE AUGER ELECTRON APPEA--ETC(U)
MAR 77 M DEN BOER, P I COHEN, R L PARK

N00014-75-C-0292

NL

UNCLASSIFIED

1 OF 1
AD
A038680



END

DATE

FILMED

5-77

AD A 038680

12

OFFICE OF NAVAL RESEARCH

Contract No. N00014-75C-0292

TECHNICAL REPORT

ELASTIC AND INELASTIC CONTRIBUTIONS TO THE
AUGER ELECTRON APPEARANCE POTENTIAL SPECTRUM OF TITANIUM

by

Marten den Boer, Philip I. Cohen and Robert L. Park
Department of Physics and Astronomy
University of Maryland
College Park, Maryland 20742

March 28, 1977

Submitted to Surface Science


Reproduction in whole or in part is permitted for
any purpose of the United States Government

DISTRIBUTION OF THIS DOCUMENT IS UNLIMITED

AD No. _____
DDC FILE COPY

DDC
RECEIVED
APR 22 1977
D

REPORT DOCUMENTATION PAGE		READ INSTRUCTIONS BEFORE COMPLETING FORM
1. REPORT NUMBER N00014-75C-0292	2. GOVT ACCESSION NO.	3. RECIPIENT'S CATALOG NUMBER
4. TITLE (and Subtitle) ELASTIC AND INELASTIC CONTRIBUTIONS TO THE AUGER ELECTRON APPEARANCE POTENTIAL SPECTRUM OF TITANIUM		5. TYPE OF REPORT & PERIOD COVERED Technical Report
7. AUTHOR(s) Marten den Boer, Philip I. Cohen and Robert L. Park		6. PERFORMING ORG. REPORT NUMBER
9. PERFORMING ORGANIZATION NAME AND ADDRESS Department of Physics and Astronomy University of Maryland College Park, Maryland 20742		8. CONTRACT OR GRANT NUMBER(s) N00014-75C-0292
11. CONTROLLING OFFICE NAME AND ADDRESS Office of Naval Research 800 N. Quincy Street Arlington, Virginia 22217		10. PROGRAM ELEMENT, PROJECT, TASK AREA & WORK UNIT NUMBERS 11/28 Mar 77
14. MONITORING AGENCY NAME & ADDRESS (if different from Controlling Office)		12. REPORT DATE March 28, 1977
		13. NUMBER OF PAGES 22
		15. SECURITY CLASS. (of this report) Unclassified
		15a. DECLASSIFICATION/DOWNGRADING SCHEDULE
16. DISTRIBUTION STATEMENT (of this Report) Approved for public release; distribution unlimited 219 638		
17. DISTRIBUTION STATEMENT (of the abstract entered in Block 20, if different from Report)		
18. SUPPLEMENTARY NOTES Technical report, submitted for publication in <u>Surface Science</u>		
19. KEY WORDS (Continue on reverse side if necessary and identify by block number) Surfaces, Titanium, appearance potentials, secondary electrons, Auger electrons		
20. ABSTRACT (Continue on reverse side if necessary and identify by block number) The energy distribution of electrons contributing to the L-shell Auger electron appearance potential spectrum of a polycrystalline titanium surface has been measured. The Auger electron appearance potential spectrum is obtained by differentiating the total secondary electron yield of an electron bombarded sample as a function of incident electron energy. At the threshold for scattering from a core level the secondary yield increases. Most of the electrons contributing to this increase have (cont.)		

20. Energies below 30 eV, and result from secondary processes following Auger recombination of the core hole. The elastic yield decreases at the threshold, however, due to opening a new channel for inelastic scattering. A comparison of the elastic yield spectrum (DAPS), the total yield spectrum (AEAPS) and the soft X-ray yield spectrum (SXAPS), shows very similar line shapes, but differences in the relative strength of the lines.
- 

FORM 100	WHEN SECTION	<input checked="" type="checkbox"/>
	OUT SECTION	<input type="checkbox"/>
		<input type="checkbox"/>
DISTRIBUTION/AVAILABILITY CODES		
AVAIL. AND/OR SPECIAL		
A		

Elastic and Inelastic Contributions to the
Auger Electron Appearance Potential Spectrum of Titanium[†]
by

Marten denBoer, Philip I. Cohen and Robert L. Park
Department of Physics and Astronomy
University of Maryland
College Park, Maryland 20742

ABSTRACT

The energy distribution of electrons contributing to the L-shell Auger electron appearance potential spectrum of a polycrystalline titanium surface has been measured. The Auger electron appearance potential spectrum is obtained by differentiating the total secondary electron yield of an electron bombarded sample as a function of incident electron energy. At the threshold for scattering from a core level the secondary yield increases. Most of the electrons contributing to this increase have energies below 30 eV, and result from secondary processes following Auger recombination of the core hole. The elastic yield decreases at the threshold, however, due to opening a new channel for inelastic scattering. A comparison of the elastic yield spectrum (DAPS), the total yield spectrum (AEAPS) and the soft X-ray yield spectrum (SXAPS), shows very similar line shapes, but differences in the relative strengths of the lines.

[†]This work was supported by the Office of Naval Research under Grant N00014-75C-0292.

INTRODUCTION

Appearance potential spectroscopy measures the threshold potentials for the creation of excited core states of atoms in the surface region of a solid. Fine structure above the excitation edges is related to the density of unfilled states. In the soft X-ray appearance potential technique^{1,2} the total X-ray yield of an electron bombarded sample is measured as a function of incident electron energy. Differentiation enhances the threshold structure relative to a smoothly rising bremsstrahlung background. Soft X-ray appearance potential spectroscopy (SXAPS) has found use in recent years primarily as a high-resolution core level probe of the electronic structure of the surface region.

In the energy range of interest for surface studies (< 2000 eV) an excited core state is much more likely to decay by an Auger process than by emission of an X-ray photon. Early attempts to identify these thresholds, however, were indecisive. Farnsworth³ concluded that correlations of inflections in the secondary yield with the critical potentials for X-ray production were fortuitous. Richardson,⁴ on the other hand, reported that, although there were many unexplained inflections in the secondary electron yield, the yield increased at every potential for which an increase in soft X-ray emission could be detected. This structure is extremely weak, and difficult to identify in the total yield. But although weak, these thresholds are quite sharp and may be detected in the derivative of the secondary electron yield.^{5,6} This technique has been termed Auger electron appearance potential spectroscopy (AEAPS).

A similar procedure that also examines excitation thresholds has been used by Kirschner and Staib^{7,8} in a technique to which they refer as Disappearance Potential Spectroscopy (DAPS). In this technique one measures changes in only the elastic secondary electron yield. Although

the total secondary emission may increase at an excitation threshold, the elastic scattering coefficient decreases because of the availability of a new channel for inelastic scattering. This technique appears to be somewhat more surface sensitive than AEAPS,⁸ but a thorough comparison has not been made. These two techniques sample different energy ranges of secondary electrons and their detailed understanding requires a knowledge of the change in the distribution of secondary electrons as an excitation threshold is crossed.

The distribution of electrons contributing to the AEAPS signal is also relevant to efforts to interpret Auger electron spectroscopy (AES) quantitatively. To interpret the measured line shapes of Auger signals requires a knowledge of the secondary emission from electron sources inside the material. We believe that the energy distribution of the electrons contributing to the AEAPS signal gives considerable insight into these secondary emission processes.

In the present paper we present a study of the energy distribution of the electrons contributing to the L_3 ($2p\ 3/2$) and L_1 ($2s$) Auger electron appearance potential spectrum of a polycrystalline Ti surface. It will be shown that most of the electrons have energies below about 30 eV, but that the details of the distributions are different for different excitation thresholds. In addition, we compare L-shell spectra measured by DAPS, AEAPS, and SXAPS.

EXPERIMENTAL

Auger electron appearance potential spectroscopy is ordinarily carried out with a simple triode arrangement in which the sample forms the anode, and the sample current is differentiated.⁹ In this form AEAPS is the simplest of all core level spectroscopies. To determine

the energy distribution of electrons contributing to the spectrum, however, we have employed a 2π spherical grid retarding analyzer shown schematically in Figure 1. Electrons impinge on the sample surface at normal incidence and are backscattered into a nearly field-free region. A small positive bias is maintained on the first grid to avoid space charge problems. Analysis is performed by the second and third grids, which are connected together. They function as a high pass filter that serves to reject electrons of energy less than eV_a , where V_a is the potential of the grids relative to the sample. A fourth grid is commonly used as a capacitive shield, but is not required if the potential modulation is superimposed on either the sample or the gun filament.

For AEAPS the analyzing potential is set at zero to pass all secondaries. The 2π collector measures essentially all secondaries which are not scattered directly back into the electron gun. For DAPS the analyzing grid is biased with respect to the electron source rather than ground. The bias, V_r , is generally set a few volts positive with respect to the filament, to pass only elastically and quasi-elastically scattered electrons. For the experiments described here, however, the effect of increasing the bias to pass more secondaries was examined. In both the DAPS and AEAPS measurements, the collected electrons pass through the same grids, and relative measurements should be unaffected by transmission losses.

Because the secondary electron background is poorly behaved in both AEAPS and DAPS, it is generally better to make measurements in the second derivative rather than the first. This is done by detecting the second harmonic of the modulation frequency. The incident electron energy is modulated by superimposing a small sinusoidal oscillation (~ 0.1 V r.m.s.)

on the accelerating potential. The spectrum is obtained by plotting the amplitude of the second harmonic variation of the collector current, as the primary electron energy eV_0 is ramped. The resolution, which is typically .5 eV, is limited by the spread in incident electron energy, with slight additional broadening from the oscillation amplitude.

Slight variations in the circuitry allows the Auger electron spectrum (AES) or characteristic loss spectrum (CLS) to be obtained. For these purposes the gun potential V_0 is fixed at some arbitrary value, well removed from any appearance potentials. The spectra are obtained by ramping the potential on the analyzing grids and again plotting the amplitude of the second harmonic content of the collector signal. For characteristic loss spectra the modulation is superimposed on the filament potential. This has the effect of selecting signals correlated with the incident electron energy.¹⁰ To obtain the Auger electron spectrum the modulation is applied between the sample and ground. This effectively discriminates against features correlated with the incident electron energy.

The Auger electron spectrum of the polycrystalline titanium sample used in this study is shown in Figure 2. Traces of carbon and oxygen impurities are evident on the surface. The sample was cleaned by argon-ion sputtering and annealing. Some argon remains imbedded in the sample after a brief anneal. Extended annealing, however, resulted in a diffusion of sulfur to the surface. The base pressure in the stainless steel bell jar system was below 10^{-10} Torr. The Auger spectrum gave no evidence of contamination from background gases over periods much longer than was required to obtain the data.

A polycrystalline sample was selected to reduce the effect of diffraction on the secondary electron yield.¹¹ On the polycrystalline sample, the diffraction related variations damp out rather quickly, and in the vicinity of the L-shell spectrum (450 - 560 eV) background variations are not a serious problem.

RESULTS

Titanium's L-shell Auger electron appearance potential spectrum (AEAPS) is shown together with its disappearance potential spectrum (DAPS) in Fig. 3. In AEAPS, the second derivative of the total secondary electron yield was obtained with the analyzer grids at ground potential ($V_a = 0$). In DAPS, the second derivative of the quasi-elastic component of the secondary electron yield was obtained with the analyzer grids set to pass only electrons that had lost no more than 5 eV with respect to the incident electron energy.

The most obvious difference between the AEAPS and DAPS spectra is that the signals are 180° out of phase. This means that the number of true secondary electrons produced by the decay of the core hole exceeds the number of elastically reflected electrons lost to the excitation process. This is not a result that could have been anticipated with any certainty. Indeed, it may well prove not to be the case for all levels of all materials.

A clearer understanding of the processes involved can be obtained by considering the energy distribution of the secondary electrons contributing to the AEAPS spectrum. This distribution can be obtained by comparing the secondary electron energy distribution measured with the primary electron energy just below a given threshold for core level excitation with that measured when the primary energy is just above the

threshold. In practice this comparison is made by measuring the amplitude of the appearance potential spectrum as a function of the potential on the analyzing grids.

The results for the L_3 and L_1 appearance potential spectra are shown in Fig. 4. The plots were taken in two parts. Below 300 V, the potential on the analyzing grids (V_a) was applied with respect to the sample, and the modulation was imposed on the sample potential (Fig. 1). This amounts to comparing the "turned-on" and "turned-off" distributions lined up at zero kinetic energy. The characteristic loss features, however, are shifted in energy by the modulation. This produces large artifacts when the analyzer potential begins to cut off the characteristic loss features. To compare the turned-on and turned-off distributions at high energies therefore, the analyzing grids were biased with respect to the filament and the modulation was imposed on the filament potential. This has the effect of comparing the turned-on and turned-off distributions matched at the elastic peak.

The L_3 ($2p_{3/2}$) plot was taken by ramping the potential on the analyzing grids with the primary electron energy set to coincide with the first maximum of the L_3 appearance potential spectrum. Similar results are obtained by setting on any other feature of the spectrum.

The L_1 (2s) appearance potential spectrum was too weak to permit a continuous plot of its amplitude as a function of analyzer potential. Its amplitude was therefore measured point by point as indicated by the open circles in Fig. 4.

Positive values in Fig. 4 correspond to the case in which the collector current increases at the threshold for core excitation. Thus, more secondary electrons are gained from the decay of the core hole than are lost

due to its creation. As the analyzing grid potential (V_a) is increased, secondary electrons with energies less than eV_a are rejected. Therefore, the amplitude decreases.

At only about 25 V, the L_3 appearance potential spectrum is effectively cancelled. As the potential on the analyzing grids is further increased, the spectrum reappears inverted. The initially rapid decrease means that most of the electrons contributing to the L_3 Auger electron appearance potential spectrum have energies below about 30 eV (making correction for the work function of the analyzing grids).

This might at first seem surprising, since it is clear from the Auger electron spectrum in Fig. 2 that the principal Auger peaks resulting from radiationless recombination of the L_3 hole have energies in the neighborhood of 400 eV. The explanation, of course, is that many Auger electrons are inelastically scattered before escaping from the sample. The number of emitted low-energy secondary electrons resulting from this inelastic scattering, greatly exceed the number of Auger electrons that escape without inelastic collisions.

Some idea of the energy distribution of electrons emitted as a result of a particular Auger transition, could be gained from an examination of the secondary electron energy distribution resulting from the impact of monoenergetic electrons from an external source. Such a distribution for the polycrystalline titanium sample used in these studies is shown in Fig. 5. The spectrum was taken in two parts. The part labelled "emission" corresponds to those features of the secondary electron energy distribution that are uncorrelated with the energy of the incident electrons. The emission spectrum results from the decay of excited states created by stopping the incident electron beam. The electrons contributing to the emission spectrum are sometimes called the "true" secondary electrons.

The contribution labelled "loss" represents those features of the secondary electron energy distribution that are correlated in energy with the incident electrons, and hence represents elastically scattered electrons, plus those electrons that have suffered discrete energy losses in the creation of excited states. Normally, the secondary electron energy distribution is given by the sum of the emission and loss spectra.

A particular Auger transition will result in a somewhat similar spectrum: an elastic peak representing the full energy of the ejected electrons; a number of characteristic loss features; and a large low energy peak. The proportions of these contributions will be different, however, since the Auger electrons originate from a distribution of internal sources. Thus, the rapid decrease of the appearance potential signal with analyzer potential simply means that for internal Auger sources, as with external beams of electrons, most of the emitted electrons are contained in the true secondary maximum at low energies.

The derivative of the plot of appearance potential amplitude as a function of analyzer potential in Fig. 4 should provide us with the energy distribution of electrons contributing to the appearance potential spectrum, but this is a rather different sort of distribution. The distribution has a large true secondary peak at low energies, and a sharp elastic peak at the high energy limit. However, the change in true secondaries contributes to an increased yield above the threshold, whereas the change in elastic yield produces a decrease in total yield. Therefore, the derivative of Fig. 4 would more nearly resemble the difference between the emission and loss portions of the secondary electron energy distribution (Fig. 5), than their sum.

The overall shape of the distribution of electrons contributing to the L_1 Auger electron appearance potential spectrum is similar to that of the L_3 , but is shifted upward. As a result it does not cross zero until about 325 V, indicating a much smaller relative elastic contribution. This is also evident in Fig. 3, in which the strength of the 2s disappearance potential spectrum is much weaker relative to the 2p, than is the case for the Auger electron appearance potential spectrum. There is of course no reason to expect the relative elastic and inelastic contributions to the yield to be the same for all levels. The difference in this case is at least partially attributable to the $2p \rightarrow 2s$ Coster-Kronig transition. Thus the recombination of a 2s hole should produce the same distribution of emitted electrons as recombination of a 2p, plus those secondaries associated with the Coster-Kronig transition.

A comparison with the soft X-ray appearance potential spectrum of the same levels is of interest. SXAPS measures the increase in X-ray yield on crossing the threshold for excitation of a core hole.^{1,2} The strong $2p \rightarrow 2s$ transition nonradiatively transfers the 2s hole to the 2p level. The excitation of the 2s (L_1) level is therefore signalled by an increase in the yield of X rays essentially identical to that for excitation of a 2p. Therefore, the soft X-ray appearance potential spectrum should accurately reflect the relative excitation probabilities of the L_3 and L_1 levels.

The DAPS, AEAPS and SXAPS spectra of the titanium L-shell are compared in Fig. 6. The spectra were taken using the same sample. The DAPS and AEAPS spectra were taken under essentially identical conditions. The SXAPS spectrum, however, required a much higher primary current, and hence some sample heating was involved. The modulation amplitude was the same for all three techniques, but a different electron source was used for SXAPS

and hence the resolution may have been slightly different. The modulation amplitude was increased somewhat over that used for Fig. 3, to reduce the integration time.

The line shapes in all three techniques are similar, although small differences can be seen. These differences may relate to the fact that DAPS and AEAPS examined a small region of the surface, while the incident electrons in SXAPS were spread over a much larger area. Our point here, however, is that the strength of the 2s spectrum relative to the 2p, is about the same for AEAPS and SXAPS, whereas for DAPS the 2s is relatively much weaker. Thus, AEAPS appears to accurately reflect the relative excitation probabilities of the levels. The reasons for the relative weakness of the 2s disappearance potential spectrum is not understood.

DISCUSSION

It is clear from the comparison of SXAPS, AEAPS and DAPS that all three spectroscopies provide essentially the same information. The high primary currents required in SXAPS, however, create serious problems. These high currents are necessitated by low fluorescence yields for soft X rays and poor detection efficiency. Conventional metal photocathodes, such as the one used to obtain the plot in Fig. 6, typically have quantum efficiencies for soft X rays of 10^{-2} . Using a more sophisticated soft X-ray detector, consisting of a surface-barrier detector and an aluminum filter, Anderson, et. al.¹² have been able to reduce the primary current by at least an order of magnitude. This has enabled them to follow spectral changes produced by strongly chemisorbed gases.¹³

Even with perfect detectors, however, the sensitivity of SXAPS is limited by the low fluorescence yields in the soft X-ray region. These yields are typically about 10^{-2} . Therefore it is not surprising that, for a given signal-to-noise ratio, Auger electron appearance potential spectroscopy requires much lower primary electron currents than SXAPS in any form.

Sensitivity, however, is not generally limited by signal-to-noise ratio, but by the signal-to-background ratio.¹⁴ The background in AEAPS and DAPS is poorly behaved. It is well known that at low energies the secondary electron yield is modulated by diffraction effects.¹⁵ Depending on the crystallinity of the sample, this structure may persist to several hundred eV,¹¹ particularly for materials with high Debye temperatures. This diffraction structure is the chief obstacle to the application of AEAPS and DAPS to chemisorption studies. Experiment suggests, however, that the diffraction effects are contained largely in the elastic signal. It may therefore be possible to reduce this effect by measuring just the inelastic signal.

For chemisorption studies the incident electron beam in AEAPS and DAPS can be defocussed to further reduce the current density at the surface. Since the resolution of appearance potential spectrometers is fixed by the spread in incident electron energies, a defocussed electron beam creates no difficulty. Indeed, the simplest way to obtain the AEAPS spectrum is to differentiate the sample current.

It would appear from Fig. 3 that although the 2p AEAPS signal is larger than the DAPS, the signal-to-noise ratio is lower. This is not surprising. The shot noise in the AEAPS spectrum is contributed by the

total secondary yield, whereas in DAPS only the much smaller elastic yield contributes. The situation is just reversed for the 2s spectrum however. The 2s signal is proportionately so much smaller in DAPS that the signal-to-noise ratio is greater for AEAPS. Thus it seems that no simple rules based on signal-to-noise ratio can be stated to assist in choosing between these techniques. As is so often the case, it is probably best to have both.

REFERENCES

1. R. L. Park and J. E. Houston, J. Vac. Sci. Technol. 11, 1 (1974).
2. R. L. Park, Surface Science 48, 80 (1975).
3. H. E. Farnsworth, Phys. Rev. 31, 405 (1928).
4. O. W. Richardson, Proc. Roy. Soc. London A119, 531 (1928).
5. R. L. Gerlach, Surface Science 28, 648 (1971).
6. J. E. Houston and R. L. Park, Phys. Rev. B 5, 3808 (1972).
7. J. Kirschner and P. Staib, Phys. Lett. 42A, 335 (1973).
8. J. Kirschner and P. Staib, Appl. Phys. 6, 99 (1975).
9. R. L. Park, M. denBoer and Y. Fukuda, Proceedings of the 6th Czechoslovak Conference on Electronics and Vacuum Physics, Bratislava, 1976 (to be published).
10. R. L. Gerlach, J. E. Houston and R. L. Park, Appl. Phys. Lett. 16, 179 (1970).
11. M. denBoer, Y. Fukuda and R. L. Park, paper presented at the International Conference on the Physics of X-ray Spectra, August 30, 1976, National Bureau of Standards, Gaithersburg, Md.
12. S. Andersson, H. Hammarqvist and C. Nyberg, Rev. Sci. Instrum. 45, 877 (1974).
13. S. Andersson and C. Nyberg, Solid State Comm. 15, 1145 (1974);
S. Andersson and C. Nyberg, Surface Science 52, 489 (1975).
14. R. L. Park in Experimental Methods in Catalytic Research Vol. III, ed. R. B. Anderson and P. T. Dawson (Academic Press, New York 1976).
15. E. G. McRae and C. W. Caldwell, Surface Science 57, 63 (1976).

FIGURE CAPTION:

1. Schematic diagram of the Spectrometer. The secondary electrons from an electron beam at normal incidence to the sample are analyzed and collected with hemispherical grids. To obtain the second derivative of the collector current, a small modulation is superimposed on the incident beam energy and the second harmonic is detected. With the switch in position "a", only those secondaries with energy greater than eV_a are collected. $V_a = 0$ corresponds to an AEAPS measurement (total yield.) With the switch in position "d", only those secondaries that have an energy less than eV_r below the primary are collected. V_r adjusted to admit only those electrons in the elastic peak corresponds to a DAPS measurement (elastic yield).

2. The Auger electron spectrum of the polycrystalline Ti sample. The excitation beam energy is 1600 eV. The sample surface was prepared by Ar ion bombardment and annealing.

3. Elastic (DAPS) and total yield (AEAPS) spectra of the Ti 2p and 2s levels. The total yield increases at the threshold for core level excitation while the elastic yield decreases. Apart from this inversion, their shapes are essentially identical.

4. Amplitude of the second derivative appearance potential signal from the 2p (solid curve) and 2s (open circles) core levels of Ti as a function of the analyzer retarding potential. To avoid artifacts, above 300 V the sample potential was modulated with respect to the analyzer grid and gun filament. Below 300 V, the gun filament potential was modulated with respect to the sample and analyzer. The resulting curves represent the integrated energy distribution of electrons contributing

to the 2p and 2s signals. The analyzer voltages corresponding to the AEAPS and DAPS modes are indicated on the 2p curve. The AEAPS spectrum was taken at zero analyzer voltage and the DAPS spectrum with a 5 V bias with respect to the gun filament.

5. Secondary electron energy distribution resulting from a 450 eV electron beam at normal incidence to the Ti sample. The distribution is divided into "emission" and "loss" parts. In the loss part the primary energy is modulated so that only features correlated in energy with the primary beam, such as the elastic and characteristic loss peaks, are detected. In the emission part, the sample potential is modulated so that only features uncorrelated with the primary energy are measured. It consists of electrons arising from decay of excited states in the metal. These include the "true" secondary peak and Auger electrons.

6. Comparison of the DAPS, AEAPS, and SXAPS spectra of the Ti 2p and 2s levels. The second derivative signal is plotted vs. the accelerating potential (the primary energy apart from a work function correction). The spectra measured by the three techniques are very similar in shape though the disappearance spectrum is opposite in sign. The amplitude of the DAPS 2s feature is much weaker relative to the 2p than is the case for either AEAPS and SXAPS. The DAPS and AEAPS spectra can be taken with much smaller incident currents, I_s , and shorter integration times, T.C., than are required for comparable SXAPS spectra.

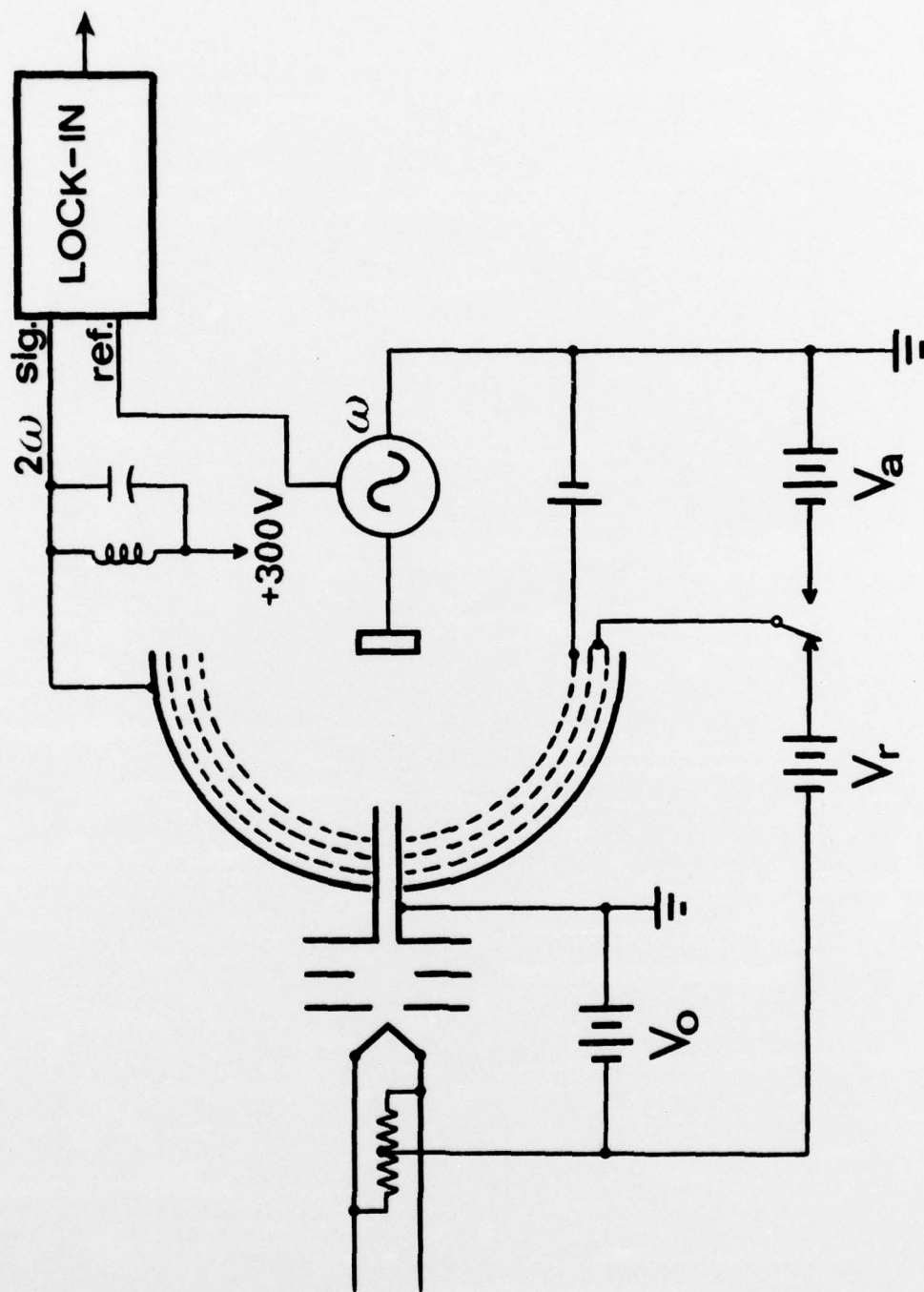


fig. 1 on 200, 201.

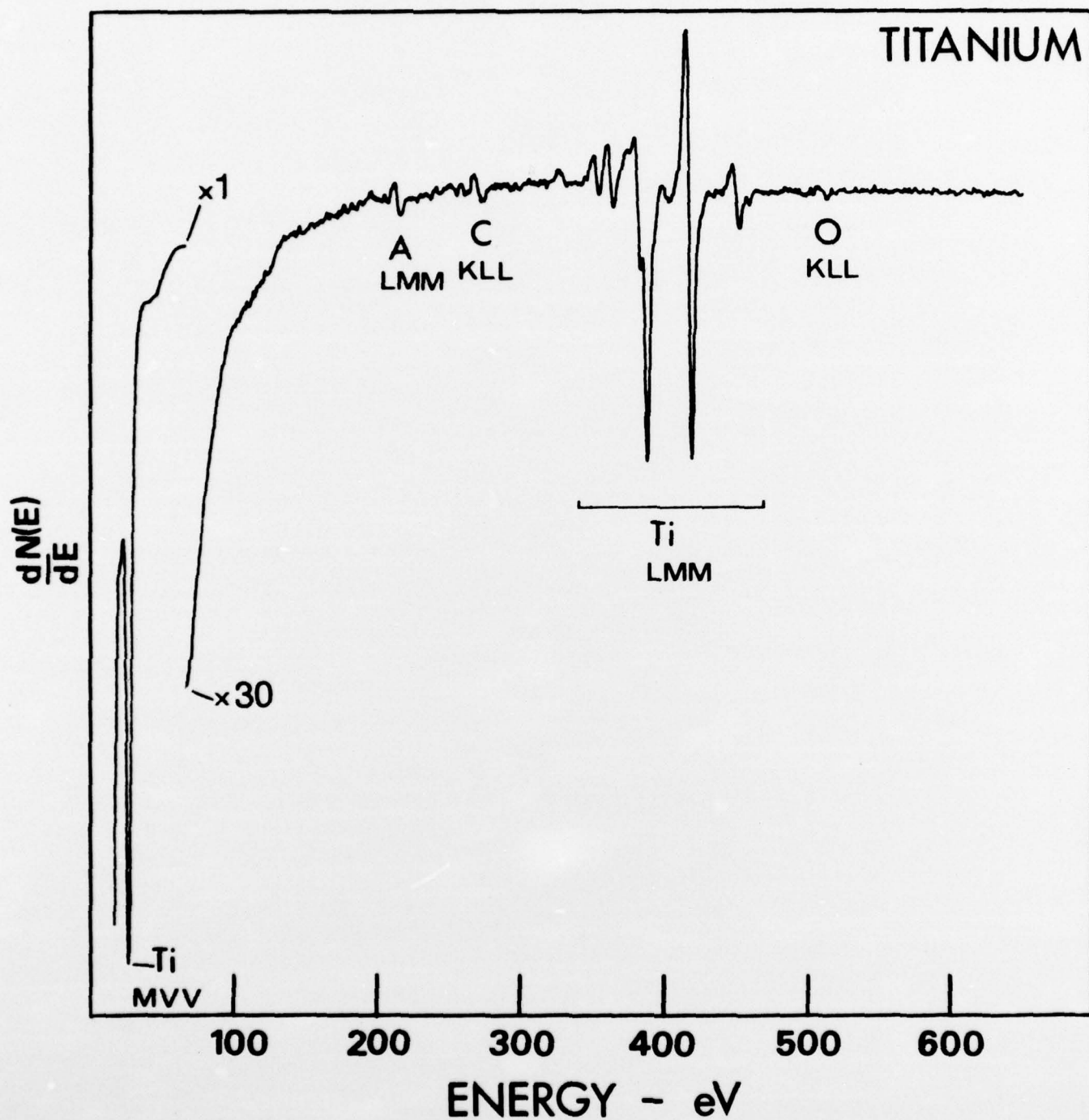
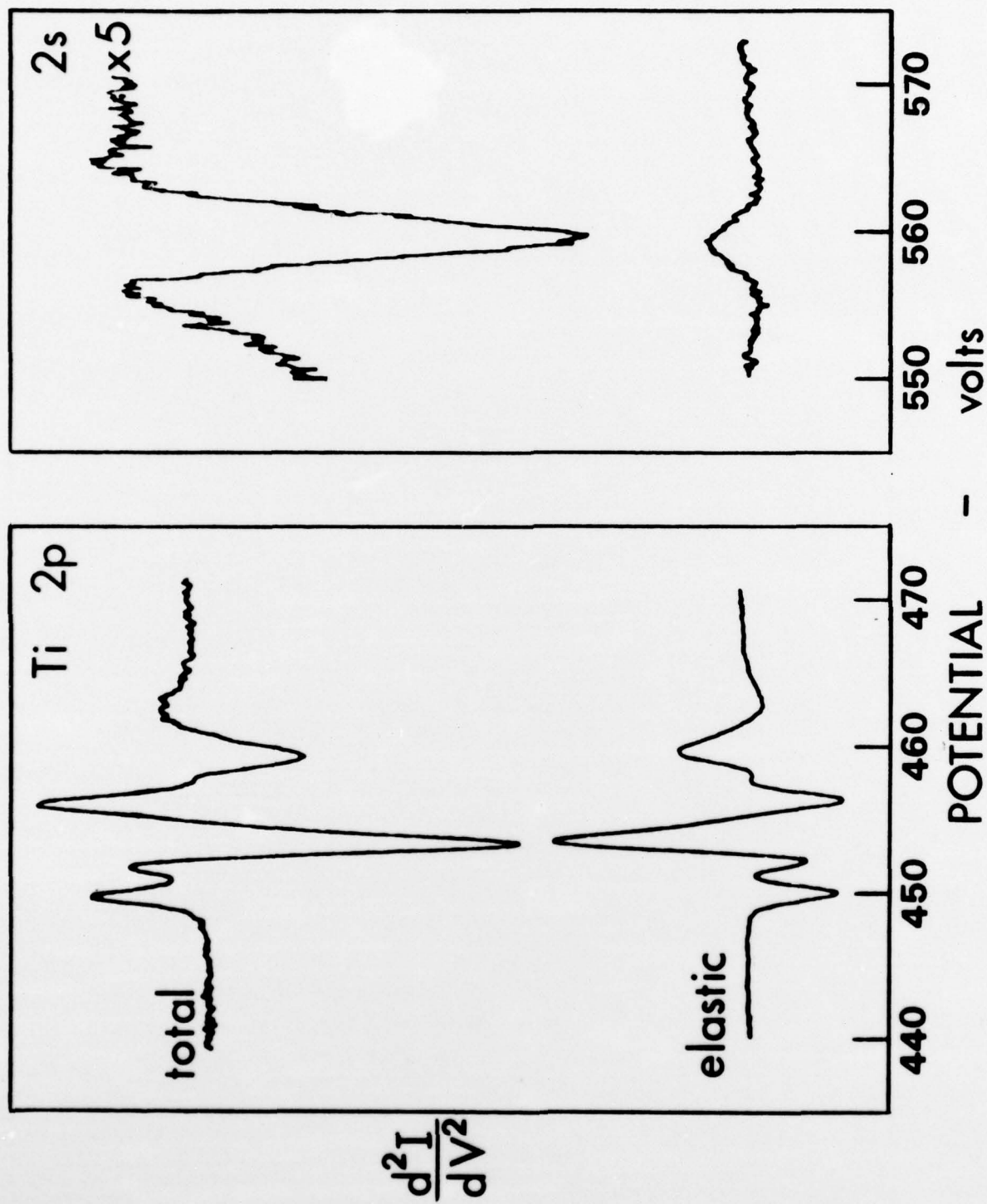


fig. 2 donkers, et al



Lin 3 den 200 17.5

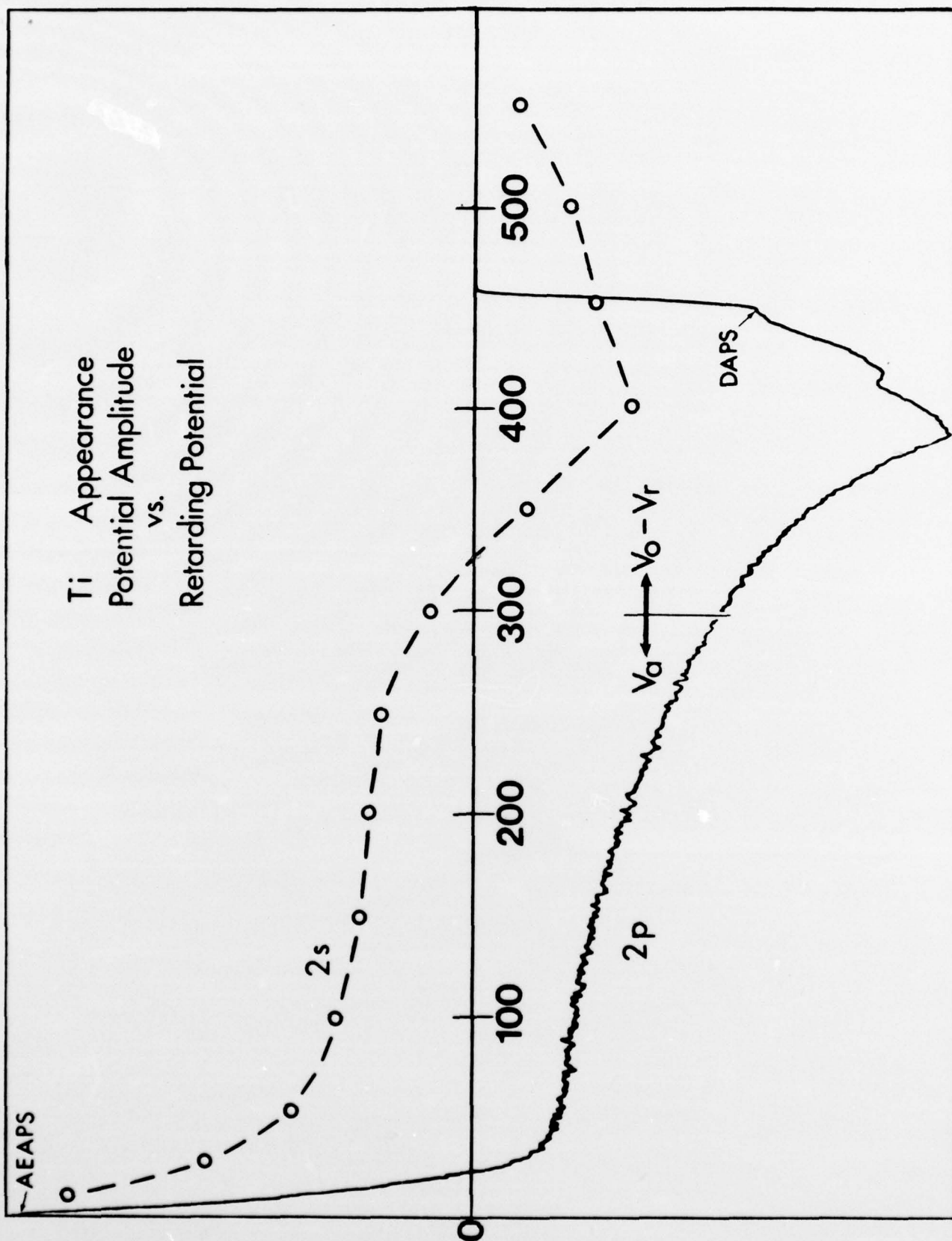


Figure 4 de. Pore, et al.

POTENTIAL - volts

Titanium

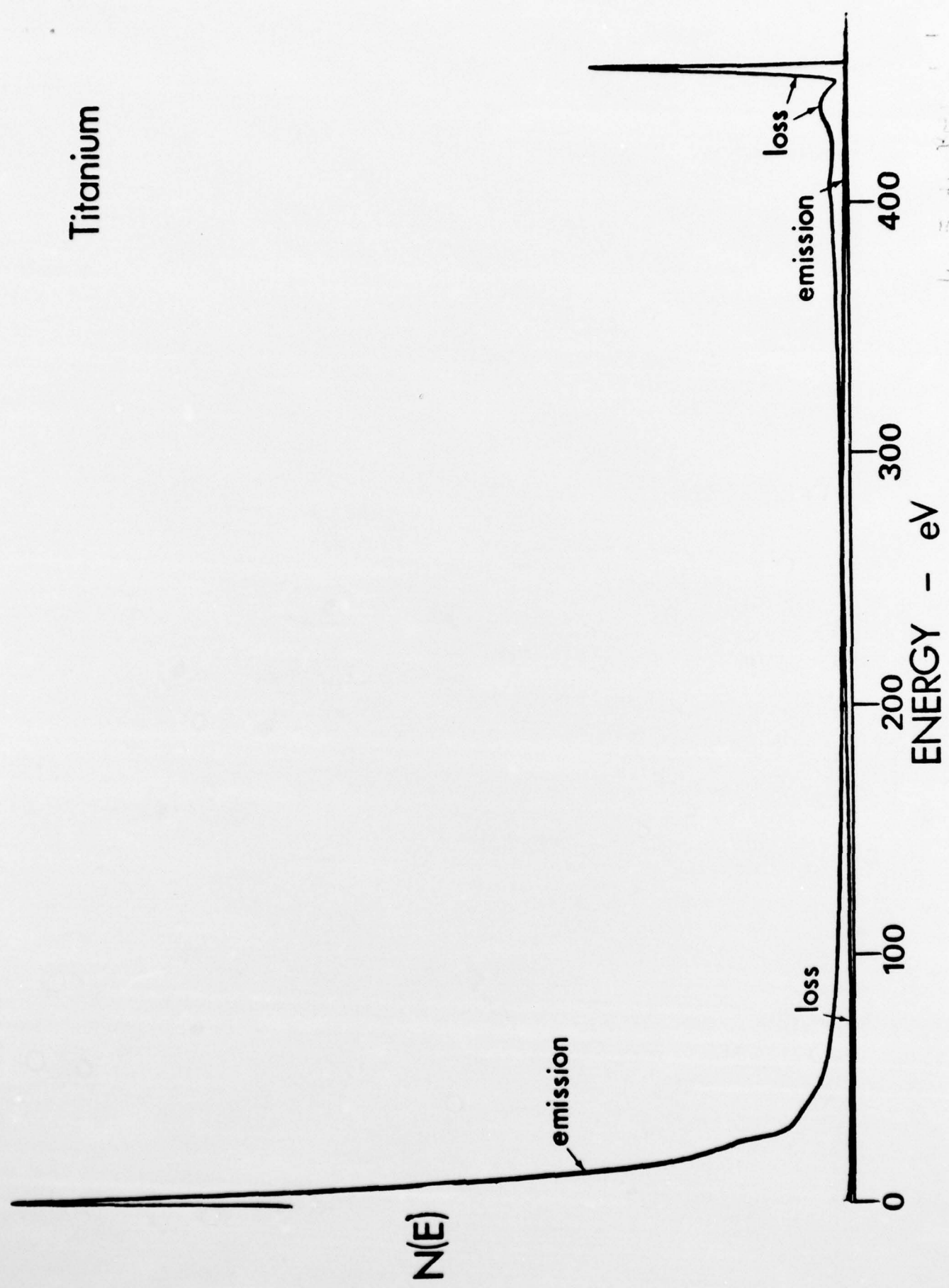
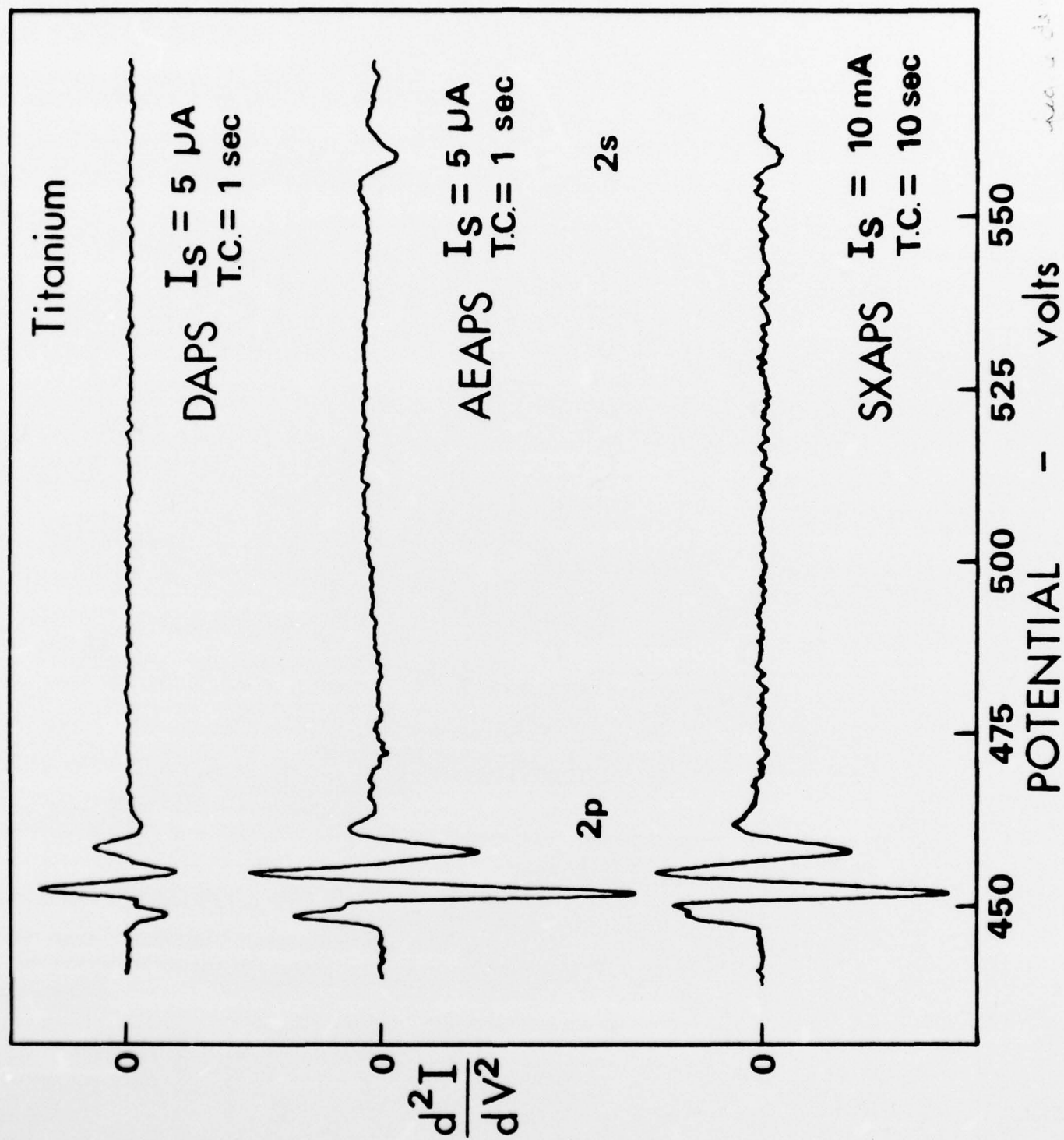


fig 5.6 b



inc. - 1000 - 10000